

## Contactless Suspension and Propulsion of Glass Panels by Electrostatic Forces

Jong Up Jeon\*, Kyu Yeol Park\*, and Toshiro Higuchi\*\*

\*School of Mechanical and Automotive Engineering, University of Ulsan, Ulsan, Korea  
(Tel : +82-52-259-2139; E-mail: jujeon@ulsan.ac.kr)

\*\*Department of Precision Machinery Engineering, University of Tokyo, Tokyo, Japan  
(Tel : +81-3-5841-6449; E-mail: higuchi@intellect.pe.u-tokyo.ac.jp)

**Abstract:** In the manufacture of liquid crystal display devices, there is a strong demand for contactless glass plate handling devices that can manipulate a glass plate without contaminating or damaging it. To fulfill this requirement, an electrostatic transportation device for glass plates is proposed. This device can directly drive a glass plate and simultaneously provide contactless suspension by electrostatic forces. To accomplish these two functions, a feedback control strategy and the operational principle of an electrostatic induction motor are utilized. The stator possesses electrodes which exert electrostatic forces on the glass plate and are divided into a part responsible for suspension and one for transportation. To accomplish dynamic stability and a relatively fast suspension initiation time, the structure of the electrode for suspension possesses many boundaries over which potential differences are formed. In this paper, an electrode pattern suitable for the suspension of glass plates is described, followed by the structure of the transportation device and its operational principle. Experimental results show that the glass plate has been transported with a speed of approximately 25.6 mm/s while being suspended stably at a gap length of 0.3 mm.

**Keywords:** Electrostatic forces, electrostatic suspension, transportation device, glass plates

### 1. INTRODUCTION

In thin glass plate related industries, particularly in the manufacture of liquid crystal display (LCD) devices, glass plates are mainly being handled through direct mechanical contact. However, for the glass panels used in LCD devices, there is an ongoing trend that their surface area is becoming larger for the purpose of increasing the through-put and decreasing the manufacturing costs. In addition, the thickness of glass panels is becoming smaller in order to minimize the weight of these devices. Consequently, their surface area/thickness ratio is becoming larger and, hence, manipulation by physical contact may lead to structural deformation or even damage. Furthermore, it is obvious that physical contact with the glass panels leads to surface contamination and particle generation which restricts the product quality. Thus, there is a strong necessity to develop contactless handling systems for glass plates.

A magnetically suspended transporter [1] and stepping actuator [2] have been studied for use in ultra-high vacuum and clean-room environments. However, these actuators can not handle glass plates directly since magnetic forces can not exert forces on them. Therefore, in order to manipulate a non-ferromagnetic object such as a glass plate, additional devices to support it are needed. This leads to direct mechanical contact resulting in surface contamination of the glass plate and particle generation. Electrostatic suspension provides us with a solution since various types of materials, such as conductive materials, semiconductors and dielectric materials, can be suspended directly by electrostatic forces.

Electrostatic suspension has already been utilized to achieve contactless support of an aluminum rotor in vacuum gyros [3]. It has also been used to support a rotor in microbearings where the rotor is a microscope cover slip on which copper is evaporated [4]. In addition, silicon wafers [5] and a 3.5-inch aluminum disk [6] have been suspended by electrostatic forces as well. The authors have succeeded in suspending glass plates, which are dielectrics, by using a stator electrode whose structure possesses many boundaries over which potential differences exist [7].

A direct electrostatic levitation and propulsion system has been developed and utilized to drive a 3.5-inch aluminum [8] and an 8-inch silicon wafer [9]. In these systems, the driving

force, which is generated around the edges of the object, is obtained by switching the voltages to a number of strip-shaped electrodes. However, this system can not be utilized for the transportation of a dielectric since the forces generated around the edges are too small to drive it. Moreover, a relatively long suspension initiation time (suspension initiation time is defined as the time between application of voltages to the stator electrodes and the start of lift of the object) is required which degrades the dynamic stability of the suspension system.

In this paper, we propose a new type of transportation device which can drive a dielectric, such as a glass plate, while suspending it simultaneously. The stator electrode is designed to decrease the suspension initiation time and to improve dynamic stability. Based on the fact that glass is a highly resistive material, the driving force is obtained by forming a traveling electric field on the glass surface which is similar to ordinary electrostatic induction motors [10-11].

### 2. DESIGN OF ELECTRODE PATTERN FOR SUSPENSION OF GLASS PLATES

The principle of electrostatic force generation in a glass plate is different from that in conductors or semiconductors. In the following, we will describe the differences between them and propose an electrode pattern appropriate for the suspension of a glass plate.

#### 2.1 Suspension force generation

Fig. 1(a) shows the charge distribution on the surface of an object which is made of conductive material just after the voltages having opposite polarities are supplied to the electrodes. The electric field lines and the resultant electrostatic forces acting on the object are also shown. Since free charges inside a conductor can move freely, their distribution on the object surface facing the electrodes will be nearly uniform immediately after applying voltages to the electrodes. As a result, a fast increase of the suspension forces can be obtained when the object is a conductor.

However, when the object is a dielectric which is slightly electrically conducting (a "poor insulator"), the nature of the charging process is different from a conductor. Since glass is

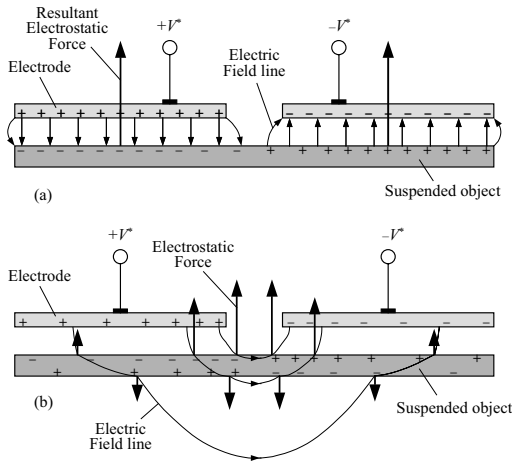


Fig. 1 Distribution of electric charge, electric field lines and electrostatic forces. (a) for conductors and (b) for dielectrics.

highly resistive, interior free charges may not move rapidly after application of voltages to the electrodes. Consequently, as shown in simulated result of Fig. 1(b) only polarization will occur in glass and polarization charges will appear on the glass surface. These polarization charges along with the induced charges on the electrodes will form an electric field causing electrostatic forces to be exerted on the glass plate. Here, the net suspension force can be obtained by subtracting the forces acting on the lower surface of the glass plate from the forces acting on its upper surface. Unless this net force is greater than the weight of the glass plate, start of suspension will not occur. Since glass is slightly conductive, the process of induction of free charges on the glass surface will be progressing gradually and thus increasing the suspension force gradually as well. From Fig. 1(b), it can be observed that the electric field in the vicinity of the boundary of the electrodes is relatively stronger than that in the region far away since the path of the electric field lines in the former is shorter. This implies that the collection process of induced charges occurs more fast in the vicinity of the boundary. As a conclusion, in order to obtain a rapid increase of suspension force and hence reduction of suspension initiation time, it is advantageous to form many boundaries, over which potential differences exist, in the electrode pattern. An alternative explanation for the fast charging process can be given by considering the charging time constant. Fig. 2 shows an one-degree of freedom model of the suspension system and its equivalent electrical circuit. It is clear that the charging time constant of this system is  $RC/2$ . By dividing each upper electrode into  $n$  smaller segments, both capacitance  $C$  and resistance  $R$  will be  $n$  times smaller, so that a smaller charging time constant and thus a fast increase of suspension force is obtained.

As evidenced from above, a dynamic relation, that includes a time delay function, exists between the applied electrode voltages and electrostatic forces. This time delay may destabilize the suspension system [7]. It is clear that a rapid

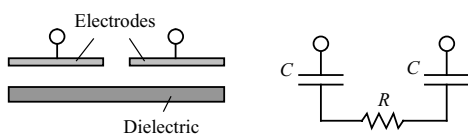


Fig. 2 One-degree of freedom model of suspension system and its equivalent electrical circuit.

collection process of free charges, in response to the application of voltages to the electrodes, will result in short time delays. Therefore, apart from a rapid increase of suspension forces, formation of many boundaries in the electrode pattern will yield a greater relative stability. Note that the distributions of charges, electric field lines and electrostatic forces at steady state, when the process of charge induction has completed, will be the same as that in conductors, which is shown in Fig. 1(a).

## 2.2 Point of application of equivalent concentrated force

In order to simplify the modeling of electrostatic suspension systems, the distributed forces generated by the stator electrodes are substituted by equivalent concentrated forces. In case of conductors, a nearly homogeneous electric field is formed in the gap between the electrodes and the object since the ratio of the overlapping area of the electrode and the object, and the gap length is large. It follows that the force density over the object surface is nearly uniform allowing the point of application of the equivalent force, which is located at the geometrical center of the electrodes as shown in Fig. 1(a), is time-invariant. In contrast to this, the force density over the dielectric surface is time-varying and non-uniform as mentioned previously until the induction process has finished. Owing to this fact, even though depending on the electrode patterns, the point of application of the equivalent force which can be different from the geometrical center point of the electrodes can be time-varying. This results in the complicated modeling of the suspension system. Therefore, electrode patterns for dielectrics suspension should be designed such that the point of application of the equivalent force is time-invariant and possibly located at the center of the electrode.

## 2.3 Restriction force generation

It is known that for objects made of conductive material, lateral restriction forces are generated due to the edge effect [12]. However, in case of objects made of slightly conductive material, e.g., glass, lateral restriction forces are generated not only at the edges but also in the vicinity of the boundaries of those electrodes having a potential difference. Fig. 1(a) shows the induced charge distribution for a slightly conductive dielectric in steady state when the induction process has finished. These induced charges will not be relaxed immediately in the event of a lateral displacement of the object with respect to the stator electrodes. As a result, as shown in Fig. 3, a spatial shift between the induced charges on the electrodes and on the object surface will arise around the boundary. This shift is responsible for the generation of lateral restriction forces around the boundary. The same situation also will arise around the edges. Clearly, the lateral restriction forces and hence the lateral dynamic stiffness can be increased by forming many boundaries in the electrode structure. Note that the principle of restriction force generation is the same as that of motive forces in induction motors.

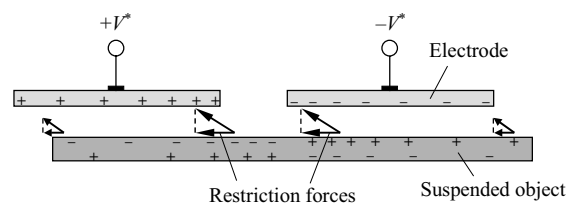


Fig. 3 Lateral restriction forces.

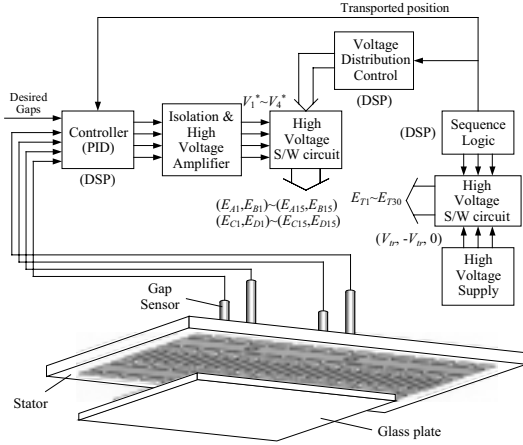


Fig. 4 Structure of the transportation system.

### 3. STRUCTURE OF TRANSPORTATION DEVICE

Fig. 4 shows the structure of the transportation device. The controller structure is divided into two distinctive parts: one part that is responsible for a stable suspension of the suspended object and one for driving the suspended object. The controller part for stable suspension consists of a stabilizing controller, high-voltage amplifiers, a voltage distribution control unit and a high-voltage switching circuit. The controller part that generates the driving forces consists of high-voltage supplies, a sequence logic control unit and a high-voltage switching circuit. The stabilizing controller, voltage distribution control unit and sequence logic control unit are implemented on a DSP system. The object to be transported is a polished soda-lime glass plate measuring  $100 \times 100 \text{ mm}^2$  and has a 0.7 mm thickness and 17.6 g mass. To measure the gap lengths between the stator electrode and the glass plate, four fiber optical gap sensors are mounted on the stator.

#### 3.1 Stator electrode

Fig. 5 depicts the stator electrode pattern. The electrodes-for-suspension  $E_{A1} \sim E_{A15}, E_{B1} \sim E_{B15}, E_{C1} \sim E_{C15}, E_{D1} \sim E_{D15}$  are interconnected as designated in Fig. 5 using dot lines. For notational convenience, a pair of interconnected electrodes is referred to in the following fashion  $(E_{A1}, E_{B1}), \dots, (E_{C15}, E_{D15})$ . The electrodes  $E_{G1}$  and  $E_{G2}$  are grounded while the electrodes  $E_{A1} \sim E_{A15}, E_{B1} \sim E_{B15}, E_{C1} \sim E_{C15}, E_{D1} \sim E_{D15}$  are supplied with the actively controlled voltages  $V_j^*$ , where  $j=1, 2, 3, 4$ . Based on this voltage supply distribution, potential

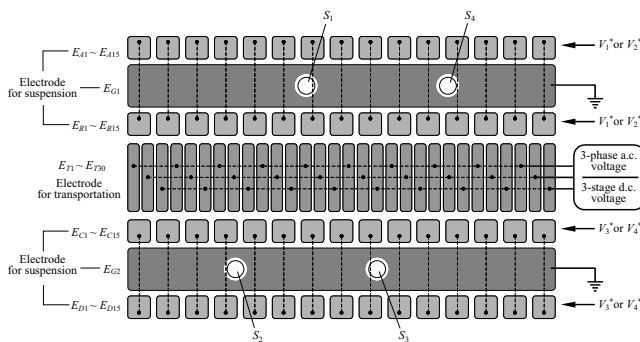


Fig. 5 Stator electrode pattern.

differences are formed over boundaries between  $E_{A1} \sim E_{A15}$  and  $E_{G1}, E_{B1} \sim E_{B15}$  and  $E_{G1}, E_{C1} \sim E_{C15}$  and  $E_{G2}$ , and  $E_{D1} \sim E_{D15}$  and  $E_{G2}$ , which leads to a decrease of the suspension initiation time and to an improvement of dynamic stability of the suspension system. In addition, we can assume that the point of application of the equivalent concentrated force is time-invariant since the structure of the electrodes and boundary regions has a symmetrical form and hence the induction process will proceed in a symmetrical manner. On the other hand, since boundaries are formed along the transportation direction, an increase of lateral restriction forces along the direction perpendicular to the transportation direction will occur. Electrodes  $E_{A1} \sim E_{A15}, E_{B1} \sim E_{B15}, E_{C1} \sim E_{C15}, E_{D1} \sim E_{D15}$  have a tooth pitch of 10.22 mm, a tooth width of 8 mm and a tooth length of 8 mm. The size of electrodes  $E_{G1}$  and  $E_{G2}$  is  $150 \times 15 \text{ mm}^2$ .

The electrodes-for-transportation  $E_{T1} \sim E_{T30}$  have a uniform tooth pitch and are connected to form three phases as shown in Fig. 5. The tooth pitch, width and length are 5.11 mm, 4 mm, and 24 mm, respectively.

#### 3.2 Controller for stable suspension

To stabilize the glass plate's movement, we need to control its motion in six degrees of freedom. Among them, the movements in the horizontal plane and the rotational motion are passively stabilized through restriction forces [12]. The remaining vertical, pitching and rolling motions are actively controlled by a feedback control strategy [6].

Fig. 6 shows the block diagram of the stabilizing controller. The gap lengths between the stator electrodes and the glass plate are measured using displacement sensors. Subsequently, the error signals for the vertical, pitching and rolling movements are computed from the measured gap lengths and the desired position/attitude signals. When transforming the measured gap lengths to the position/attitude signals, each component of the transformation matrix is recomputed depending on the position of the glass plate. The error signals are then fed back to a PID (Proportional-Integral-Derivative) compensator and control voltages in each degree of freedom are generated. These control voltages are then transformed to stator electrode control voltages by a pre-compensator which decouples the glass plate motion in each degree of freedom. After being added to the four bias voltages, the electrode control voltages are sent to the limiter. Note that a limitation is imposed on the stator voltages to prevent electric discharge which is caused by the breakdown of the electric field.

The voltages from the stabilizing controller are amplified by high-voltage amplifiers, which have an amplification ratio of 1000, and fed into a high-voltage switching circuit. Based on the information from the voltage distribution control unit, voltages  $V_j^*$ , where  $j=1, 2, 3, 4$ , are then distributed to the electrodes-for-suspension which are positioned directly above the glass plate.

#### 3.3 Controller for generation of driving force

D.c. high voltages  $V_{Tr}, -V_{Tr}$  and 0 are generated by

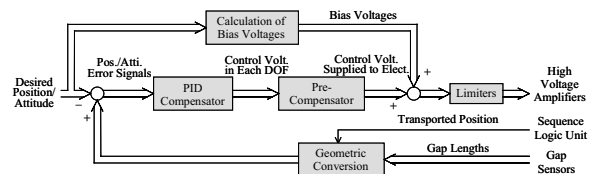


Fig. 6 Stabilizing controller.

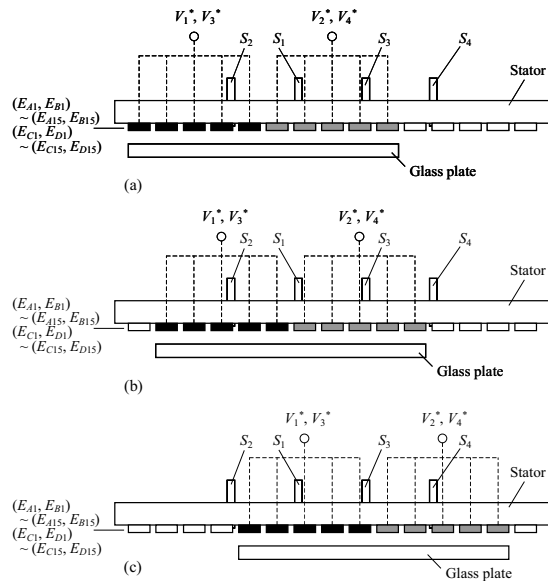


Fig. 7 Transportation process. (a) suspension step, (b) transportation step, (c) sensor change step.

high-voltage power supplies and sent to the high-voltage switching circuit. These voltages are then supplied to the electrodes-for-transportation  $E_{T1} \sim E_{T30}$  in a sequence that is controlled by the sequence logic control unit. The sequence logic control unit sends the information on the position of the glass plate to the stabilizing controller and voltage distribution control unit.

## 4. OPERATIONAL PRINCIPLE

### 4.1 Stable suspension

Based on the gap lengths detected by gap sensors  $S_1, S_2$ , and  $S_3$ , voltages  $V_1^*, V_2^*, V_3^*, V_4^*$  for stabilizing the motion of the glass plate are generated. By supplying these voltages to those electrodes-for-suspension which are positioned right above the glass plate, the glass plate can be supported contactless: voltages  $V_1^*, V_2^*, V_3^*$  and  $V_4^*$  are supplied to electrodes  $(E_{A1}, E_{B1}) \sim (E_{A5}, E_{B5}), (E_{A6}, E_{B6}) \sim (E_{A10}, E_{B10}), (E_{C1}, E_{D1}) \sim (E_{C5}, E_{D5}),$  and  $(E_{C6}, E_{D6}) \sim (E_{C10}, E_{D10}),$  respectively, as shown in Fig. 7(a). Electrodes  $E_{G1}$  and  $E_{G2}$  are grounded as mentioned before.

### 4.2 Driving process

The glass plate is driven by forming a traveling electric field on it. The traveling electric field is generated by supplying three-stage d.c. voltages, i.e.,  $V_{II}, -V_{II}, 0$  sequentially to the electrodes-for-transportation  $E_{T1} \sim E_{T30}$ , which is the driving principle of the electrostatic film actuator developed by Egawa et al. [13]. Three-phase a.c. voltages can also be utilized to generate a traveling electric field. However, in this case three high-voltage amplifiers, which are relatively costly components, are needed.

### 4.3 Switching of voltage to electrode-for-suspension

As shown in Fig. 7(b), if the glass plate is advanced one pitch of the electrodes-for-suspension, voltages  $V_2^*$  and  $V_4^*$  are supplied to electrodes  $(E_{A11}, E_{B11})$  and  $(E_{C11}, E_{D11}),$  respectively, and voltages to electrodes  $(E_{A1}, E_{B1})$  and  $(E_{C1}, E_{D1})$  are cut. Simultaneously, the voltage to electrodes  $(E_{A6}, E_{B6})$  and  $(E_{C6}, E_{D6})$  are switched from  $V_2^*$  to  $V_1^*$  and from  $V_4^*$  to  $V_3^*$ , respectively. This procedure is repeated each instant

that the glass plate is advanced one pitch. In this manner, by supplying voltages to those electrodes-for-suspension that are positioned right above the glass plate, a state of stable suspension can be maintained for the glass plate regardless its position.

The driving principle of our transportation device is the same as that of an induction motor implying that the transportation speed is asynchronous to the traveling speed of the electric field. Therefore, to determine the switching instants for the voltages to the electrodes-for-suspension, the glass plate's position has to be detected. However, from our experiments, the transportation speed of the glass plate was verified to be almost the same as (a little smaller than) the traveling speed of the electric field. For this reason, no detection system was employed in the transportation system. The switching frequency of the voltages to the electrodes-for-suspension is half that of the voltages to the electrodes-for-transportation.

## 4.4 Sensor switching

As the glass plate is advanced further and arrives at the position shown in Fig. 7(c), it is impossible to obtain the position/attitude of the glass plate since gap sensor  $S_2$  is not able to detect the gap length. In this event, the position/attitude of the glass plate can be obtained by using gap sensor  $S_4$  instead of  $S_2$ .

## 5. EXPERIMENTAL WORK

### 5.1 Experimental apparatus

Fig. 8(a) shows the schematic diagram of the experimental apparatus. Leveling of stator electrode and setting of initial gap length between stator electrode and glass plate can be performed by adjusting the upper and lower micrometer positioning screws. The stator electrodes are etched from a 35  $\mu\text{m}$  thick copper layer on a glass-epoxy base. Fig. 8(b) shows a photograph of the stator.

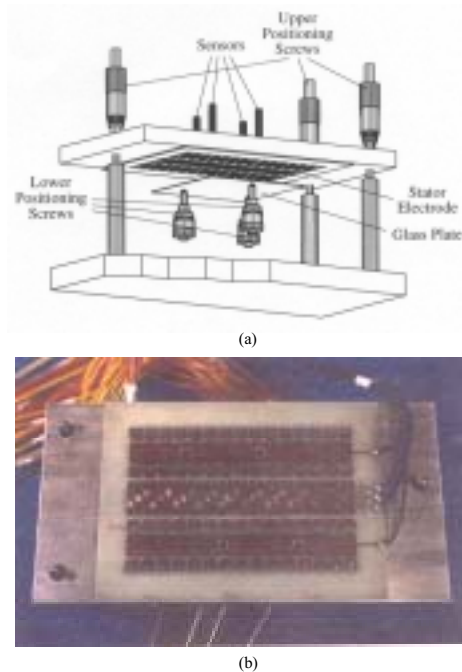


Fig. 8 Transportation process. (a) suspension step, (b) transportation step, (c) sensor change step.

## 5.2 Suspension experiments

Prior to transportation, suspension experiments were carried out with a soda-lime glass plate. In these experiments, to implement our suspension system more easily the control system parameters were derived by assuming the glass plate as a conductor [6], which gives us their approximate values. Finally the control system parameters were tuned by manual. Table 1 shows the experimental conditions including the control system parameters. Only voltages with positive polarity were supplied to the electrodes-for-suspension. The control sampling time was 100  $\mu$ s.

Table 1 Experimental conditions: \*vertical motion, \*\*pitching and rolling motion.

Parameters	Value
Proportional gains [kV/m*, kV/rad**]	1.5E5*, 40**
Derivative gains [kVs/m*, kVs/rad**]	125*, 0.025**
Integral gains [kV/m/s*, kV/rad/s**]	5E5*, 500**
Desired gap length [mm]	0.3
Bias voltages [kV]	1.61
Limit voltages [kV]	2.4
Voltages for transportation [kV]	0.9/-0.9/0
Environmental humidity [%RH]	45

Fig. 9 shows the gap length variations measured by sensors  $S_1$ ,  $S_2$  and  $S_3$  and the variations of the voltages supplied to the electrodes-for-suspension after the PID compensator was switched on. It shows that a period of time of approximately 14 seconds was needed before the glass plate started its lift from the initial gap length of 0.35 mm. As mentioned in section 2, this suspension initiation time can be decreased more by forming more boundaries in the electrodes-for-suspension. On the other hand, the suspension initiation time is strongly dependent on the environmental humidity. This is related with the fact that the characteristics of charge induction depend on the surface resistivity of glass while surface resistivity is influenced by the humidity. As the humidity increases, surface resistivity decreases so that charge induction time and hence suspension initiation time decreases.

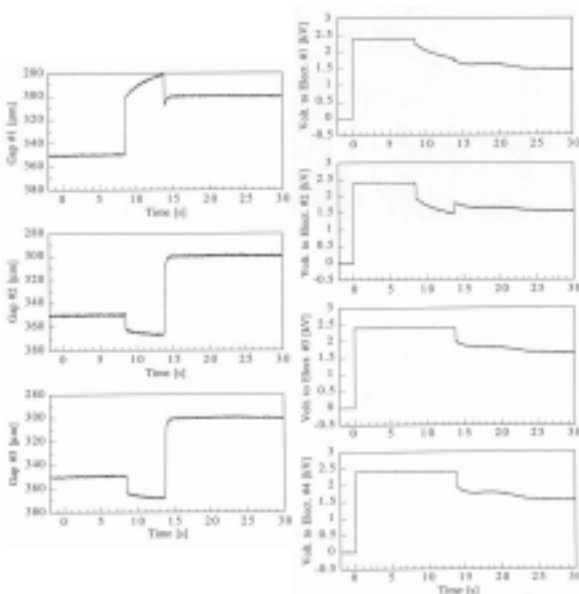


Fig. 9 Gap and voltages during suspension process.

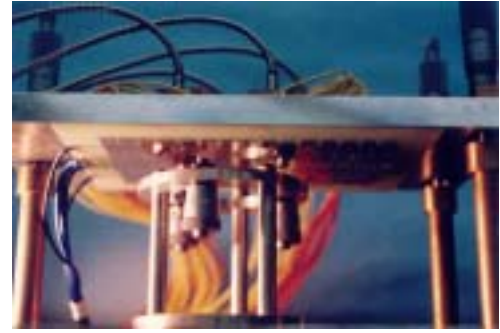


Fig. 10 Glass plate during contactless suspension and transportation.

It was found experimentally that for a humidity variation from 70 %RH to 30 %RH, surface resistivity varied from  $10^{12} \Omega$  to  $10^{17} \Omega$  and suspension initiation time varied from 1 second to 1 minutes. The data shown in Fig. 9 was recorded under an air humidity of 45 %RH.

Fig. 9 shows that during the state of stable suspension, the actively controlled voltages were slowly decreasing. A physical explanation for this drift phenomenon is that the charge built-up on the glass surface had not yet reached a steady state and indicates that the process of charge accumulation was progressing continuously during suspension. The voltages after 30 seconds from the control start were 1.48 kV, 1.55 kV, 1.64 kV and 1.57 kV, respectively. Fig. 10 shows a photograph of the glass plate under stable suspension.

## 5.3 Transportation experiments

The glass plate was driven by supplying three-stage d.c. voltages of 0.9 kV, -0.9 kV and 0 sequentially to the electrodes-for-transportation after a stable suspension was reached. Fig. 11 shows step movements recorded for a switching time of 4 seconds for the three-stage d.c. voltages. The step movements were measured by using a laser displacement sensor; a sensor target with cylindrical shape is attached beneath the glass plate and a laser displacement sensor detects its movement. The instant that the sensor was switched from  $S_2$  to  $S_4$  occurred when the glass plate was transported along a distance equal to five pitches of the electrodes-for-transportation. It was observed that the step movement was nearly the same as (a little smaller than) the tooth pitch of the electrodes-for-transportation. The reason for this is that the driving force is large enough to overcome the external forces which are mainly caused by air friction since

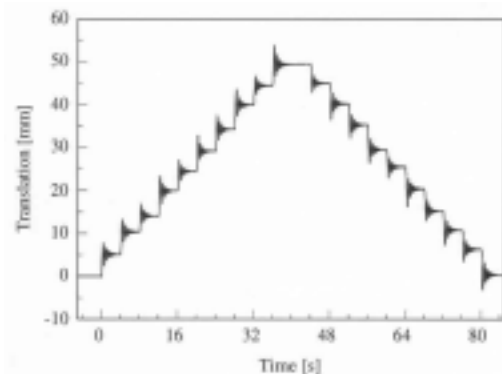


Fig. 11 Successive step movements for a switching time of 4 seconds.

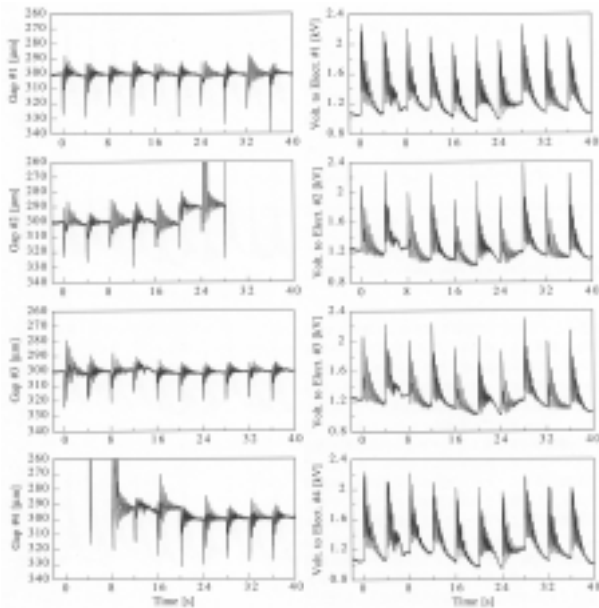


Fig. 12 Gap and voltage fluctuations during transportation process for a switching time of 4 seconds.

the glass plate is suspended contactless. Therefore, additional sensors, such as proximity switches, to detect the advanced position of the glass plate along the transportation direction were excluded in our transportation device. However, in the case that the transportation distance is long, sensors are needed since the positioning error will be accumulated and become large as the glass plate is advanced. The driving forces are strongly dependent on the surface resistivity of the object. Since the surface resistivity of glass is influenced by the environmental humidity, driving force is influenced by humidity as well. As the humidity increases, driving force decreases and thus positioning error increases. In this case, sensors are required to detect the position along the transportation direction.

Fig. 12 shows the gap length and voltage variations while the glass plate was being transported. As can be seen, the gap fluctuations were quite large at the switching instants of the three-stage d.c. voltages. The maximum amplitude of these fluctuations was approximately 30  $\mu\text{m}$ . At the instant of switching, strong repulsive forces between the charges previously induced on the glass plate and the induced charges on the electrodes were generated [13], repelling the glass plate downwards. The gap fluctuations may be decreased by using three-phase a.c. voltages instead of three-stage d.c. voltages.

## 6. CONCLUSIONS

An electrostatic transportation device for glass plates, incorporating contactless suspension of the glass plate using electrostatic forces, has been described in this paper. The transportation device features stator electrodes which are subdivided into a part responsible for suspension and one for transportation. To implement a stable suspension, the voltages supplied to the electrodes-for-suspension are actively controlled on the basis of the measured position/attitude of the glass plate. The structure of the electrodes-for-suspension possesses many boundaries over which potential differences are applied. The purpose of these boundaries is to decrease the suspension initiation time, to increase the lateral dynamic stiffness, and to improve the dynamic stability of the

suspension system. The driving forces are obtained by supplying three-stage d.c. voltages to the electrodes-for-transportation such that a traveling electric field is generated on the surface of the glass plate. The glass plates have been suspended successfully at a gap length of 0.3 mm and transported with a speed of approximately 25.6 mm/s during a state of stable suspension.

## REFERENCES

- [1] M. Ota, S. Andoh, and H. Inoue, "Mag-lev semiconductor wafer transporter for ultra-high-vacuum environment," *Proc. 2nd Int. Symp. on Magnetic Bearings*, Tokyo, Japan, pp. 109-114, 1990.
- [2] T. Higuchi, A. Horikoshi, and T. Komori, "Development of an actuator for super clean rooms and ultra high vacua," *Proc. 2nd Int. Symp. Magnetic Bearings*, Tokyo, Japan, pp. 115-122, 1990.
- [3] H. W. Knoebel, "The electric vacuum gyro," *Control Engineering*, Vol. 11, pp. 70-73, 1964.
- [4] S. Kumar, D. Cho, and W. N. Carr, "Experimental study of electric suspension for microbearings," *J. Microelectromechanical Systems*, Vol. 1, No. 1, pp. 23-30, 1992.
- [5] J. U. Jeon, J. Jin, and T. Higuchi, "Electrostatic suspension of 8-inch silicon wafer," *Proc. Inst. Electrostat. Jpn.*, Vol. 21, No. 2, pp. 62-68, 1997.
- [6] J. Jin, T. Higuchi, and M. Kanemoto, "Electrostatic levitator for hard disk media," *IEEE Trans. Industrial Electronics*, Vol. 42, No. 5, pp. 467-473, 1995.
- [7] J. U. Jeon and T. Higuchi, "Electrostatic suspension of dielectrics," *IEEE Trans. Industrial Electronics*, Vol. 45, No. 6, pp. 938-946, 1998.
- [8] J. Jin and T. Higuchi, "Direct electrostatic levitation and propulsion," *Proc. 1996 IEEE 22nd Int. Conf. on Industrial Electronics, Control, and Instrumentation*, Taipei, Taiwan, pp. 1306-1311, 1994.
- [9] J. Jin, T. C. Yih, T. Higuchi, and J. U. Jeon, "Direct electrostatic levitation and propulsion of silicon wafer," *IEEE Trans. Industry Applications*, Vol. 34, No. 5, pp. 975-984, 1998.
- [10] B. Bollée, "Electrostatic motors," *Philips Technical Review*, Vol. 30, No. 6/7, pp. 178-194, 1969.
- [11] S. D. Choi and D. A. Dunn, "A surface-charge induction motor," *Proc. IEEE*, Vol. 59, No. 5, pp. 737-748, 1971.
- [12] S. J. Woo, J. U. Jeon, T. Higuchi, and J. Jin, "Electrostatic force analysis of electrostatic levitation system," *Proc. 34th SICE Annual Conf.*, Sapporo, Japan, pp. 1347-1352, 1995.
- [13] S. Egawa and T. Higuchi, "Multi-layered electrostatic film actuator," *Proc. 1990 IEEE Micro Electro Mechanical Systems Workshop*, Napa Valley, CA, pp. 166-171, 1990.